

## Mechanical Characteristic of concentric and Eccentric Drilling Cutting Tool

Hasan AL Dabbas, Nabil M Musa, Mohammad Quqazeh.

*Department of Mechanical Engineering  
Philadelphia University - Jordan*

*Corresponding author. E-mail address: drdabbas@engineer.com*

### Abstract

In this paper cutting movement of the tilted planetary drilling is investigated. For instance, the orbital drilling strategy might be acknowledged as one of these arrangements. In any case, this system cannot abstain from machining with focus of cutting device and obliges high establishment cost. The main limitation of this method is the large difference between the diameter of the created hole and the diameter of the tool. In the paper geometrical improvement of the tool, spherical end tool has been successfully employed to facilitate electrolyte flow in the machining zone.

**Key words:** concentric, eccentric, Drilling Phase, electrolyte circulation.

### INTRODUCTION

The oil and gas industry of any country plays a vital role in building as well as strengthening its economy. The company with high oil and gas reserves certainly exhibits a strong economy. Oil and natural gas still represents the main source of energy for humankind. Apart from being an essential source of energy petroleum products, serve as a feedstock for numerous consumer goods. Hence, playing a relevant and growing role in the lives of people for this reason many countries across the globe keep on exploring new techniques and strategies for discovering oil and gas within their territories. Among different energy resources, oil and natural gas are expected to remain dominant energy resources in the prospect years. Therefore, it can be concluded that oil and gas is and will be the most crucial source of energy. Oil and gas is mainly found beneath the Earth surface and water surface. The processes involved in extracting and crude oil from both the sources are typically different in couple of ways. Therefore, drilling oil and gas can be classified into two types: Offshore drilling and onshore drilling (Amjad, 1996).

### DISCUSSION

CFRP is generally starting to be utilized as structural materials as a part of aviation and airplane commercial ventures. Nonetheless, CFRP is generally hard to machine in routine machining systems. More successful and conventional machining strategy is obliged to enhance the machinability of CFRP. For instance, the orbital drilling strategy might be

acknowledged as one of these arrangements. In any case, this system cannot abstain from machining with focus of cutting device and obliges high establishment cost. So as to enhance the circumstances, we have imagined another drilling system, which called as tilted planetary drilling.

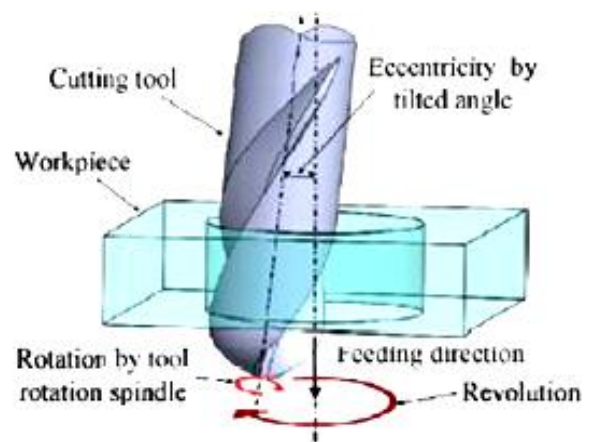


**Fig 1-Cutting tool motion of tilted planetary drilling**

Figure 1 demonstrates the cutting movement of the tilted planetary drilling. The tilted planetary drilling has two tomahawks. Because of orbital drilling, a pivot of slicing device is parallel to the hub of transformation in eccentricity. Because of the tilted planetary drilling, eccentricity is acknowledged by slant of the apparatus axle pivot. In this way, inertial swaying of transformation is decreased because tilt edge of the component is littler than eccentricity of the cutting device tip.

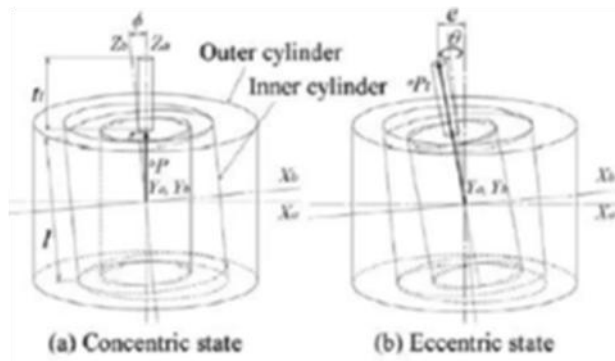


Fig -2 Eccentric tool drilling mechanism model

With a specific end goal to acknowledge accessibility of tilted planetary drilling commonsense examination of the tilted planetary drilling by utilization of a high velocity shaft unit and a machine is completed. The instrument pivot axle, which can turn autonomously, is appended to a turret apparatus holder of the machine and the work piece is settled with the toss of fundamental shaft of the machine. From the exploratory result, we could acquire drilling gaps without burr and delamination on prepared surface. In this paper, to create a model of the tilted planetary drilling is created standard model of the eccentric mechanism.

**Drilling Phase**

Once the presence of potential hydrocarbon bearing rocks is confirmed through seismic surveys the next phase is the drilling of prospect zone. In the drilling phase, the hydrocarbon bearing sedimentary rocks are drilled in order to produce oil or natural gas out of existing reserves (Agbaji, 2010, pp.1-4). The type of drilling process that should be adopted depends on the geographical formation of the area. While drilling offshore a drilling ship or submersible drilling rig or a drilling barge is required to carry out the essential activities allied with drilling of well (Eia& Hernandez, 2006 ,pp.3-6) . Once the process of drilling starts, mud or other drilling fluids are continuously circulated around the drilling bit in order to maintain an adequate hydrostatic pressure, remove the cuttings of formation and to lubricate and cool the drilling bits. This stage of production of oil or natural gas entails immense amount of hazardous waste, which is eventually discharged into the atmosphere (Chan, 1975). According to Nooman and Curtis (2003), some of the common waste produced because of drilling activities include cutting of the formation, drilling mud, excess drilling chemicals, simulation and work over fluids, non-burnable waste scrap metals and construction material. All of the stated wastes significantly contribute in environmental pollution. In fact inadequate hydrostatic pressures can lead to blowouts that immensely affect the environment (Kotchen&Burger,2007, pp.4720-4729).

**Eccentric mechanism Principle**

Figure 2 shows schematic of the eccentric mechanism. The eccentric mechanism of tilted planetary drilling framework is comprised of multi-barrel mechanism. Figure 2(a) and 2(b) demonstrates the concentric state and eccentric tilted state, individually. Outline a (X<sub>a</sub>, Y<sub>a</sub>, Z<sub>a</sub>) is Cartesian coordinate framework with root at the middle of the external chamber. Outline b (X<sub>b</sub>, Y<sub>b</sub>, Z<sub>b</sub>) is Cartesian coordinate framework with inception at the inside of the internal barrel. Outline b has tilted φ as the Y<sub>a</sub>-hub from casing a. As of right now, the device tip position vector after eccentric is characterized by the Eq. (1), where l stands for length of the internal barrel and it remains for device length and stands for separation that the hub of revolution was mapped to the top end surface from the core of the inward chamber and stands for the turn edge around the Z<sub>b</sub> of casing b.

$${}^a P_t = \begin{pmatrix} \cos \phi & 0 & \sin \phi & 0 \\ 0 & 1 & 0 & 0 \\ -\sin \phi & 0 & \cos \phi & 0 \\ 0 & 0 & 0 & 1 \end{pmatrix} \begin{pmatrix} 1 + \frac{2t_i}{l} \\ \frac{\epsilon \cos \theta}{l} \\ \frac{\epsilon \sin \theta}{l} \\ 1 \end{pmatrix} \quad (1)$$

Therefore, the center position of the tool tip and the eccentricity are as follows:

$${}^a P_t = \begin{pmatrix} (1 + \cos \theta) \left( \frac{l + 2t_i}{2} \right) \sin \phi \\ \left( \frac{l + 2t_i}{2} \right) \tan \phi \sin \theta \\ (\cos \phi - \sin \phi \tan \phi \cos \theta) \left( \frac{l + 2t_i}{2} \right) \end{pmatrix} \quad (2)$$

$$e = \sqrt{\left\{ (1 + \cos \theta) \left( \frac{l + 2t_i}{2} \right) \sin \phi \right\}^2 + \left\{ \left( \frac{l + 2t_i}{2} \right) \tan \phi \sin \theta \right\}^2} \quad (3)$$

**Calculation of the eccentricity**

Figure 3 demonstrates a 3d model characterized by CAD, and figure 4 demonstrates the estimation consequence of the eccentricity where, l is 150 mm and t<sub>i</sub> is 50 mm. Likewise, the speeding up is mimicked by utilization of the 3d model at advancement velocity is 200/min and e is 3 mm. The eccentricity which φ is 3 degrees affirmed to increment direct in the scope of 0-35 degrees and, the increasing speed is 3.8 mm/s<sup>2</sup>. At the point when φ is 2 degrees, the important reach is expanded and linearity is lost. As it were, the eccentricity can be gotten while keeping little d more when φ is 3 degrees. Additionally, the increasing speed is 3.1 mm/s<sup>2</sup> which φ is 2 degrees. There is not a noteworthy contrast. Accordingly, φ is recognized as 3 degrees.

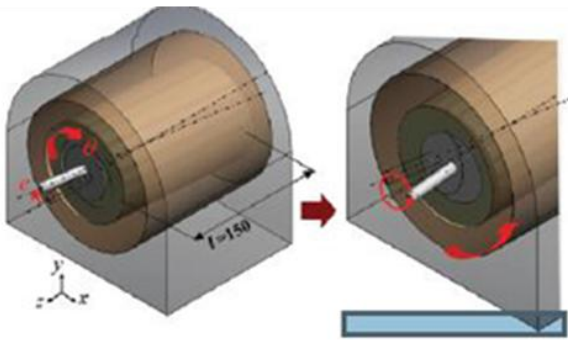


**Fig 3. 3Dmodel of eccentric mechanism**

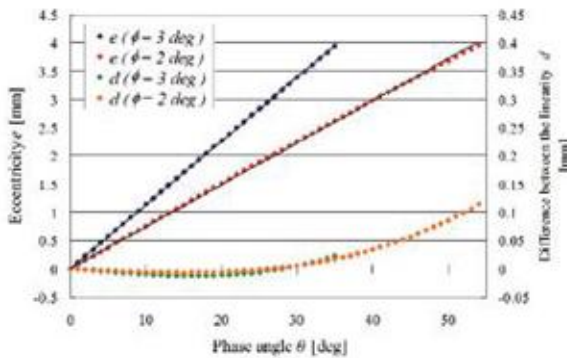


**Fig 4. Calculation result of the eccentricity**

Electrochemical discharge machining (ECDM) is a non-conventional machining method that has been firstly introduced for glass micro drilling by kurafuji and Suda. This process which has attracted extensive research interests in recent years, combines features of electrochemical machining (ECM) and electro discharge machining (EDM) with the additional advantage of machining electrically non-conductive materials. High temperature melting and thermally accelerated chemical etching enable the ECDM process to machine very hard and brittle materials including glass and ceramics in a reasonable time and cost. As demonstrated in Fig. 1, the ECDM process takes place in an electro-chemical cell using two electrodes. The tool electrode is used as cathode electrode and a counter electrode, which is greater in size in comparison with cathode, is used as the anode electrode. The two electrodes are dipped into an electrolyte solution and connected to a D.C. power supply, consequently when a voltage higher than a critical value is applied, electrolysis in the solution starts and hydrogen bubbles grow so dense on the tool electrode (cathode) that they coalesce into a gas film. The gas film acts as an insulating layer around the tool and provides electrical potential difference between the tool and electrolyte. Consequently, electrical discharges take place between tool and electrolyte. When the workpiece is in the close vicinity of the cathode, the sparks strike the work piece and cause melting or vaporizing of the struck spots and results in material removal from the work piece. Because the electrochemical discharge process is highly dependent on the availability of the electrolyte in the machining zone,

electrochemical discharge drilling with high aspect ratio faces various limitations.

In fact, the electrolyte circulation in the machining area and debris removal from this region become highly restricted as the machining depth increases (more than around 200  $\mu\text{m}$ ). So far, different approaches have been made to improve the electrolyte

Circulation and debris removal and consequently achieve higher depth in the ECDM process. In general, the approaches can be divided into two main categories including applying different tool kinematics and improving the tool shape. In addition, applying eccentric rotation to the tool has been effectively employed by some other researchers.

The main limitation of this method is the large difference between the diameter of the created hole and the diameter of the tool. In the case of geometrical improvement of the tool, spherical end tool has been successfully employed to facilitate electrolyte flow in the machining zone. In another approach, Zheng et al. utilized a flat sidewall tool for glass drilling which resulted in decrease in machining time and improvement of the geometry of the hole. Moreover, the electrolyte circulation has been improved using a micro drill tool instead of a cylindrical rod. Regarding the tool kinematics, another potential approach, which can be employed, is axial vibration of the tool. They demonstrated that applying low frequency vibration to a simple stationary cylindrical tool may reduce the machining time particularly in the hydrodynamic regime.

This approach was limited to consideration of applying sinusoidal waveform to a cylindrical tool and the effects of different waveforms and tool shapes were not studied. In this paper, the effects of applying longitudinal vibration to the two different tool shapes including cylindrical rod and micro drill are studied.

The vibrations were applied in a wide range of amplitudes and frequencies and in two different waveforms including sinusoidal and square waveforms. The effects of the mentioned parameters on the drilling speed of glass are discussed. According to the results, using vibrating tool can be considered as a proper way to enhance the material removal rate in most circumstances however, it might not be true in some cases and is highly depended on the other parameters of ECDM process.

#### Experimentation method

To conduct the experiments, an electrochemical discharge drilling setup with gravity feeding system was prepared as depicted in Fig. 2. The electrolyte chamber was filled with 700  $\text{cm}^3$  of 25 wt.% NaOH. Soda-lime glass slides of size 75 mm  $\times$  25 mm  $\times$  1 mm were selected as work piece. For gravity feeding system, a weight was employed to provide a 1 N contact force between work piece and tool. In addition, a 500  $\mu\text{m}$  diameter cylindrical rod and 500  $\mu\text{m}$  micro drill made of Tungsten carbide were used as cathode electrode and a 304 L stainless steel plate of size 100 mm  $\times$  50 mm  $\times$  10 mm was used as anode electrode. In the case of micro drill as cathode electrode, a DC motor was used to produce the required rotation. Also a DC power supply (0–60 V, 0–5 A) was employed to apply the required working voltage. In addition, a piezoelectric actuator was employed to apply the axial vibrations to the cathode electrode. The actuator works by

means of applying pulsed voltage provided by a voltage pulse generator.

Using the pulse generator, two different types of voltage waveforms were produced. In this regard, sinusoidal and square waveforms were applied to the actuator and consequently tool vibration frequencies ranging from 1 Hz to 500 Hz and vibration amplitudes ranging from 1 to 30 m were achieved.

Using a linear variable differential transformer (LVDT) the machining depth progress was monitored and stored on a PC through a data acquisition card (DAQ) with 500 Hz sampling rate. To investigate the effects of tool longitudinal oscillation on the ECDM outputs, numerous sets of experiments have been conducted. The parameters, which have been considered in this study, are listed in Table 1. The mentioned parameters were tested in all levels as depicted in Table 1 in a full factorial experimentation methodology. In addition, each experiment was repeated five times and the mean value of experiment results is reported in "Section 3".

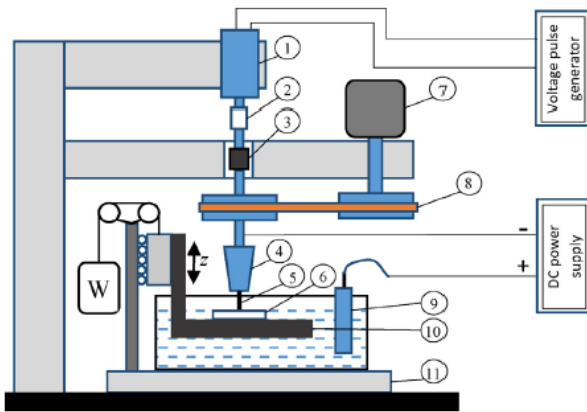


Fig 5 Schematic View of vibration assisted ECDM Setup

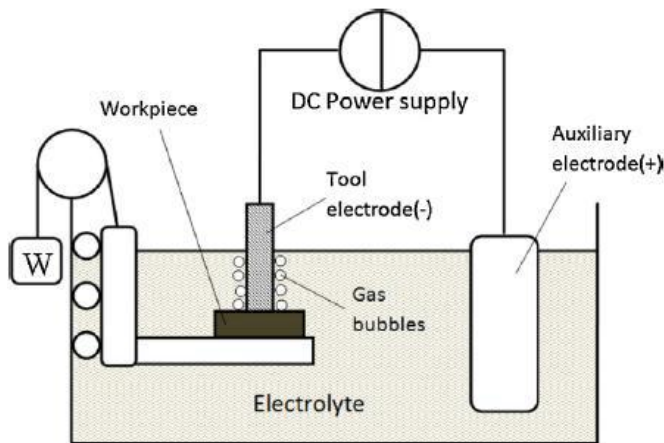


Fig 6 Schematic view of ECDM setup using gravity feeding system

Studies of Fluid Flow in Eccentric Annulus  
 Equation of Motion.

The general form of the equation of motion for a fully developed flow in a

Cartesian coordinate system is:

$$\frac{\Delta P_f}{\Delta L} + \frac{\partial}{\partial x} \left( \mu \frac{\partial v}{\partial x} \right) + \frac{\partial}{\partial y} \left( \mu \frac{\partial v}{\partial y} \right) = 0$$

The above equation is very similar to a simplified version of the Navier-Stokes equation except that the viscosity term here is not taken out of the derivative since it is only a constant for Newtonian fluids. The pressure drop is constant because of the assumption of fully developed flow.

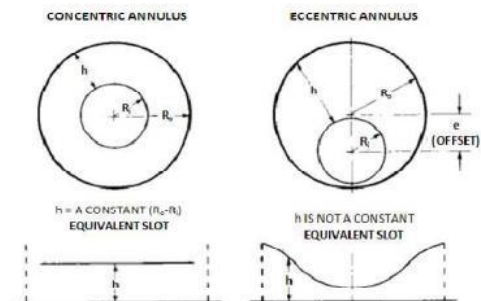
Cylindrical coordinates cannot be applied due to the asymmetric nature of an eccentric annular geometry (Fig. 2.1). Hence, a bipolar coordinate system is often adopted to describe this complex geometry. In this orthogonal coordinate system, the two cylindrical boundaries of the fluid annulus coincide with two surfaces having constant values of  $\epsilon$  ( $\epsilon_i$  and  $\epsilon_o$ , which can be expressed in terms of the annulus radius ratio  $S$  and the dimensionless eccentricity  $\xi$  as given in the nomenclature). The other coordinate ( $\eta$ ) represents a set of eccentric cylinders whose centers lie on the  $y$ -axis and which intersect orthogonally the boundaries of the fluid annulus. The transformed geometry for the fluid annulus in the complex  $\epsilon - \eta$  plane is a slab of length  $(\epsilon_i - \epsilon_o)$  and width equal to the limits of  $\eta$ , that is  $2\pi$  (Figure 2.3).  $L$  is the third axis, which is perpendicular to  $\epsilon$  and  $\eta$ . The relationships needed to transform from Cartesian coordinates to bipolar coordinates are given by (Speigel, 1968):

$$x = \frac{a \sinh \epsilon}{\cosh \epsilon - \cos \eta}$$

$$y = \frac{a \sin \epsilon}{\cosh \epsilon - \cos \eta}$$

$$L = L$$

Where  $a = R_i \sinh -i = R_o \sin \epsilon_o$ ; also,  $0 \leq \eta \leq 2\pi$  and  $-\infty \leq \epsilon \leq +\infty, -\infty \leq L \leq +\infty$



$$\frac{\partial \tau_{yz}}{\partial y} = -\frac{\partial p}{\partial z}$$

$$\frac{\partial \tau_{xz}}{\partial x} + \frac{\partial \tau_{yz}}{\partial y} = -\frac{\partial p}{\partial z}$$

Fig (7)

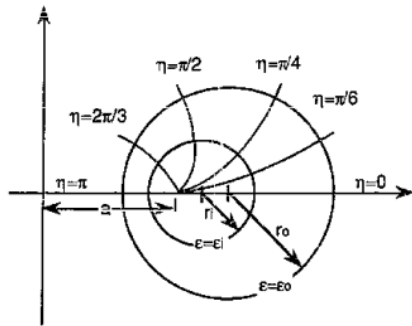
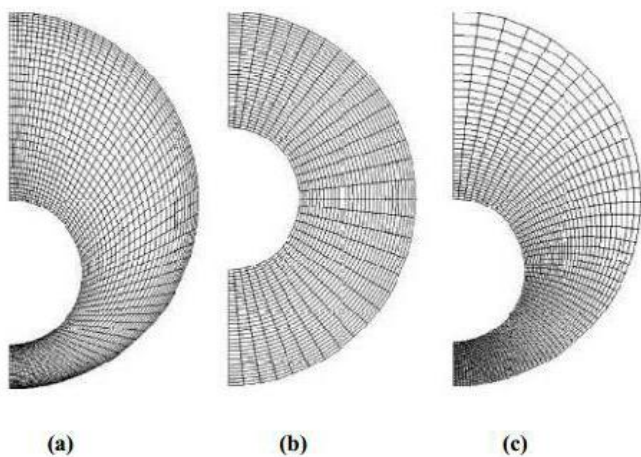


Fig (8)

At this point mention should be made of other sets of computational grids that have recently found significant application in the analysis of heat and fluid flow in eccentric annular geometries. Notable amongst them is the “boundary conforming, natural coordinates,” which is a non-orthogonal, boundary-fitted, and curvilinear coordinates system, with inbuilt ability to handle complicated geometries. For an eccentric annulus, a two-boundary technique of grid generation can be used to build such non-orthogonal curvilinear grid in physical space.

Two types of orthogonal grids are also presented in Figure 9- the polar orthogonal coordinate for the concentric annulus and the bipolar orthogonal coordinate for the eccentric annulus. Most of the recent studies have successfully utilized the non-orthogonal, boundary-fitted, and curvilinear coordinates, to analyze the flow field of non-Newtonian fluids in conduits of arbitrary cross sections, ranging from the simple case of a slightly eccentric annulus to a more tasking case of eccentric annular sections in the presence of cutting bed



Fig(9) Typical geometry and meshing of an eccentric annulus

a- Mesh system b- non- orthogonal co-ordinate c- polar orthogonal

To find simple approximations for the velocity profile and the volumetric flow rate, Tao and Donovan (1955) treated an eccentric annulus as a variable-height slot (Fig. 2.1) and developed the analytical solutions for Newtonian fluids. This assumption has been proved to work reasonably well for flows through concentric annuli (Bourgoyne et al, 1987) for certain range of tubular diameter ratio.

In their experimental and theoretical work, flow of Newtonian fluids in an eccentric annulus with and without inner pipe rotation was investigated. However, they made several simplifying assumptions that led to incorrect flow rate predictions.

Using a bipolar coordinate system and Green’s function, Heyda (1959) presented analytical solutions for Newtonian fluid flow in an eccentric annulus in the form of an infinite series. He showed that the velocity profile of Newtonian fluid in laminar flow regime would differ dramatically in an eccentric annulus. Similarly, Snyder and Goldstein (1965), using the bipolar coordinate system, determined the velocity distribution for the fully developed laminar flow of a Newtonian fluid in an eccentric annulus.

The analytical expression for the volumetric flow-rate is rather complex and was not presented by Snyder and Goldstein (1965). However, after a lengthy treatment, Tosun (1984) developed expressions for the volumetric flow-rate. Using the expressions for volumetric flow-rate in a concentric annuli developed by Bird et al. (1960), he presented the ratio of the volumetric flow rates in eccentric and concentric annuli in terms of the diameter ratio and the eccentricity, for a given pressure gradient. Their results showed that this ratio increases as the diameter ratio and the eccentricity increases.

In 1965, Vaughn (1965) extended the approach of slot flow approximation to pursue a solution of non-Newtonian Power-law fluids in eccentric annulus. However, he used the same wrong equations for variable slot height (Eq. 2.16) and the equation of motion as Tao and Donovan. Subsequently, Iyoho and Azar (1981) modified Vaughn’s approach, developing an accurate technique to calculate the variable slot height by avoiding the latter’s simplifying assumptions and developed analytical solutions of the velocity profile and the volumetric flow-rate for power-law fluids. Iyoho and Azar’s equation for variable slot height is given by;

They presented results requiring no mathematical transformation or iterative computations, which they claimed were comparable in accuracy with those obtained numerically by previous investigators using complex bipolar coordinates, and iterative computations. Subsequently, Uner. (1988) extended Iyoho and Azar’s slot-height model to approximate volumetric flow-rates for both Newtonian and non-Newtonian fluids.

They neglected Iyoho and Azar’s simplifying assumptions in computing the volumetric flow-rate by accounting for eccentricity ratio while formulating their solutions. However, they also applied the wrong equation of motion. Furthermore, Luo and Peden (1990) noted that the slot model, because it is in essence a modified model for flow

between parallel plates, will result in unrealistic symmetric profiles of the shear-stress/shear-rate magnitudes and the velocity. Consequently, they treated an eccentric annulus as being composed of an infinite number of concentric annuli with variable outer radii ( $R_o$ ), which were described as:

$$R_o^\xi = \xi \cos \theta + \sqrt{R_o^2 - [\xi \sin \theta]^2}$$

Using the velocity profile for the concentric annuli flow, they developed analytical solutions for the shear stress, shear rate, velocity, and volumetric flow rates/pressure gradient for both power-law and Bingham-plastic fluids. However, Yu (1994) reported that Luo and Peden's method failed to give accurate solutions of velocity profiles even for Newtonian fluids flowing in an eccentric annulus, because the equations of motion they used could not correctly describe the flow situation in an eccentric annulus.

The error increased as eccentricity increases. Seemingly unaware or following total negligence of the limitations of the narrow slot approximation for an eccentric annulus, Haige and Yinao (1997) developed expressions for the velocity distribution, flow-rate, and pressure drop for Robertson Stiff fluids flowing through an eccentric annulus. Though, citing the work of Iyoho and Azar, they still assumed a small clearance and ended up with the same simplified expression for variable height that was first applied by Tao and Donovan. The expression, they developed for the pressure loss is presented in Equation 2.19.

$$\Delta P = \frac{2A}{R_o - R_i} \left\{ \frac{2\bar{U} + \frac{3}{4}C \left( 2 + \frac{2e^2}{R_o + R_i} + e^2 \right)}{\frac{2B}{1+2B} (R_o - R_i) \left[ 1 + \frac{1}{4} \left( \frac{1+B}{B} \right) \frac{e^2}{R_i(R_o + R_i)} \right]} \right\}^B$$

where

A = consistency index of a Robertson-Stiff (RS) fluid, Pa.sB

B = Flow behavior index of a RS fluid, dimensionless

C = Shear rate correction index in RS model, s-1

$R_o$  = inner radius of outer cylinder, in.

$R_i$  = outer radius of inner cylinder, in.

e = offset distance between the centre of the two cylinders, in.

QR = average velocity in an eccentric annulus, ft/sec.

## Conclusion

Certainly, it seems like an acceptable notion that analytical solutions are not the way to go; hence, no new research has been reported in this area. On the other hand, numerical models continue to attract attention, boosted by the increasing memory available in today's hard drives and the processing speed of computers.

## References

[1] Amjad, M. (1996). Control of ITH percussive long hole drilling in hard rock (Order No. NQ70176). Available from ProQuest Dissertations & Theses Full Text. (304314205). Retrieved from

<http://search.proquest.com/docview/304314205?accounid=35812>

[2] Chan, P. W. K. (1975). Stress analysis of webs with eccentric holes (Order No. MK24289). Available from ProQuest Dissertations & Theses Full Text. (302815857). Retrieved from <http://search.proquest.com/docview/302815857?accounid=35812>

[3] Chapman, J. R. (2006). Behaviour of collared concrete columns under concentric or eccentric loads (Order No. MR13800). Available from ProQuest Dissertations & Theses Full Text. (304959360). Retrieved from <http://search.proquest.com/docview/304959360?accounid=35812>

[4] Cummings, C. A. (1993). A theoretical study of the flow of slightly compressible non-Newtonian fluids in eccentric annuli with entrance effects (Order No. 9315790). Available from ProQuest Dissertations & Theses Full Text. (304076515). Retrieved from <http://search.proquest.com/docview/304076515?accounid=35812>

[5] Cummings, G. D. (1978). The Interaction between The Utricles And The Semicircular Canals During Eccentric Rotation (Order No. 7816016). Available from ProQuest Dissertations & Theses Full Text. (302886272). Retrieved from <http://search.proquest.com/docview/302886272?accounid=35812>

[6] Eilers, M. G. (2012). Investigation of strength of a hybrid adhesive anchor system used in precast concrete welded repair applications subjected to tensile and eccentric shear loading (Order No. 3524148). Available from ProQuest Dissertations & Theses Full Text. (1071262441). Retrieved from <http://search.proquest.com/docview/1071262441?accounid=35812>

[7] Fang, P. (1998). Numerical investigation of laminar forced convection in Newtonian and non-Newtonian flows in eccentric annuli (Order No. 9835888). Available from ProQuest Dissertations & Theses Full Text. (304446343). Retrieved from <http://search.proquest.com/docview/304446343?accounid=35812>

[8] Iyoho, A. W. (1980). Drilled cuttings transport by Non-Newtonian drilling fluids through inclined, eccentric annuli (Order No. 8016890). Available from ProQuest Dissertations & Theses Full Text. (288091050). Retrieved from <http://search.proquest.com/docview/288091050?accounid=35812>

[9] Jo, H. (2008). Mechanical behavior of concentric and eccentric casing, cement, and formation using analytical and numerical methods (Order No. 3341623). Available from ProQuest Dissertations & Theses Full Text. (275865606). Retrieved from <http://search.proquest.com/docview/275865606?accounid=35812>

[10] Kushniruk, J. K. (1997). Vibration balancing analysis of a dual face mill eccentric grinder machine head

- (Order No. MQ30984). Available from ProQuest11Dissertations & Theses Full Text. (304373772). Retrieved from <http://search.proquest.com/docview/304373772?accountid=35812>
- [11] Miller, T. H. (1990). Behavior of cold-formed steel wall stud assemblies subject to eccentric axial loads (Order No. 9018028). Available from ProQuest Dissertations & Theses Full Text. (303826438). Retrieved from <http://search.proquest.com/docview/303826438?accountid=35812>
- [12] Motahhari, H. R. (2008). Improved drilling efficiency technique using integrated PDM and PDC bit parameters (Order No. MR44620). Available from ProQuest Dissertations & Theses Full Text. (287929506). Retrieved from <http://search.proquest.com/docview/287929506?accountid=35812>
- [13] Nguyen, T. C. (2009). Predicting dynamic barite sag in oil based drilling fluids (Order No. 3375187). Available from ProQuest Dissertations & Theses Full Text. (305005711). Retrieved from <http://search.proquest.com/docview/305005711?accountid=35812>
- [14] Ogugbue, C. C. E. (2009). Non-Newtonian power-law fluid flow in eccentric annuli: CFD simulation and experimental study (Order No. 3390067). Available from ProQuest Dissertations & Theses Full Text. (304979169). Retrieved from <http://search.proquest.com/docview/304979169?accountid=35812>
- [15] Payne, M. L. (1992). Drilling bottom-hole assembly dynamics (Order No. 9234422). Available from ProQuest Dissertations & Theses Full Text. (304011425). Retrieved from <http://search.proquest.com/docview/304011425?accountid=35812>
- [16] Pereira, J. J. (1999). Comprehensive optimization of drilling parameters for horizontal wells (Order No. 9947565). Available from ProQuest Dissertations & Theses Full Text. (304528076). Retrieved from <http://search.proquest.com/docview/304528076?accountid=35812>
- [17] Rohs, S. A. (2000). Eccentric nation: Irish embodiment and performance in nineteenth-century new york city (Order No. 9971989). Available from ProQuest Dissertations & Theses Full Text. (304611451). Retrieved from <http://search.proquest.com/docview/304611451?accountid=35812>
- [18] Satkan, C. (2013). Equivalent circulating density contribution to the plastering effect of casing while drilling technology: Analysis of annular fluid velocity and annular pressure through computational fluid dynamics (Order No. 1545654). Available from ProQuest Dissertations & Theses Full Text. (1449405230). Retrieved from <http://search.proquest.com/docview/1449405230?accountid=35812>
- [19] Schulman, P. L. (1997). The Sunday of fiction: The modern French eccentric from raymondqueneau to jean echenoz (Order No. 9728295). Available from ProQuest Dissertations & Theses Full Text. (304376687). Retrieved from <http://search.proquest.com/docview/304376687?accountid=35812>
- [20] Sundararaj, P. (1991). High strength concrete columns under eccentric load (Order No. MM74185). Available from ProQuest Dissertations & Theses Full Text. (303967197). Retrieved from <http://search.proquest.com/docview/303967197?accountid=35812>